A&A 592, A6 (2016)
DOI: 10.1051/0004-6361/201527142
© ESO 2016

Astronomy & Astrophysics
Special feature

The XXL Survey: First results

The XXL Survey

VII. A supercluster of galaxies at $z = 0.43$[⋆,⋆⋆]

E. Pompei[1], C. Adami[2], D. Eckert[3], F. Gastaldello[4], S. Lavoie[5], B. Poggianti[6], B. Altieri[7], S. Alis[14], N. Baran[9], C. Benoist[8], Y. L. Jaffé[10], E. Koulouridis[11], S. Maurogordato[8], F. Pacaud[12], M. Pierre[13], T. Sadibekova[13], V. Smolčić[9], and I. Valtchanov[7]

[1] ESO-Chile, Alonso de Cordova 3107, Vitacura, Chile
e-mail: epompei@eso.org
[2] Aix Marseille Université, CNRS, LAM (Laboratoire d'Astrophysique de Marseille), UMR 7326, 13388 Marseille, France
[3] Department of Astronomy, University of Geneva, ch. d'Ecogia 16, 1290 Versoix, Switzerland
[4] INAF–IASF-Milano, via Bassini 15, 20133 Milano, Italy Department of Physics and Astronomy, University of California at Irvine, USA
[5] Department of Physics and Astronomy, University of Victoria, 3800 Finnerty Road, Victoria, BC, Canada
[6] Osservatorio astronomico di Padova, INAF, 35141 Padova, Italy
[7] European Space Astronomy Centre, European Space Agency, PO Box 78, 28691 Villanueva de la Cañada, Madrid, Spain
[8] Laboratoire Lagrange, UMR 7293, Université de Nice Sophia Antipolis, CNRS, Observatoire de la Cote d'Azur, 06304 Nice, France
[9] Department of Physics, University of Zagreb, Bijenička cesta 32, 45 10000 Zagreb, Croatia
[10] Department of Astronomy, Universidad de Concepción, Casilla 160-C, Concepción, Chile
[11] IAASARS, National Observatory of Athens, 15236 Penteli, Greece
[12] Argelander Institut für Astronomie, Universitat Bonn, 53121 Bonn, Germany
[13] Service d'Astrophysique AIM, CEA/DSM/IRFU/SAp, CEA Saclay, 91191 Gif-sur-Yvette, France
[14] Department of Astronomy and Space Sciences, Faculty of Science, Istanbul University, 34119 Istanbul, Turkey

Received 7 August 2015 / Accepted 27 October 2015

ABSTRACT

Context. The XXL Survey is the largest homogeneous and contiguous survey carried out with *XMM-Newton*. Covering an area of 50 deg^2 distributed over two fields, it primarily investigates the large-scale structures of the Universe using the distribution of galaxy clusters and active galactic nuclei as tracers of the matter distribution.
Aims. Given its depth and sky coverage, XXL is particularly suited to systematically unveiling the clustering of X-ray clusters and to identifying superstructures in a homogeneous X-ray sample down to the typical mass scale of a local massive cluster.
Methods. A friends-of-friends algorithm in three-dimensional physical space was run to identify large-scale structures. In this paper we report the discovery of the highest redshift supercluster of galaxies found in the XXL Survey. We describe the X-ray properties of the clusters members of the structure and the optical follow-up.
Results. The newly discovered supercluster is composed of six clusters of galaxies at a median redshift $z \sim 0.43$ and distributed across $\sim 30' \times 15'$ (10×5 Mpc) on the sky. This structure is very compact with all the clusters residing in one XMM pointing; for this reason this is the first supercluster discovered with the XXL Survey. Photometric redshifts from the CFHTLS (Canada-France-Hawaii Telescope Legacy Survey) data release T0007 placed the supercluster at an approximate redshift of $z_{\rm phot} \sim 0.45$; subsequent spectroscopic follow-up with WHT (*William Herschel* Telescope) and NTT (New Technology Telescope) confirmed a median redshift of $z \sim 0.43$. An estimate of the X-ray mass and luminosity of this supercluster returns values of $1.7 \times 10^{15}\ M_\odot$ and of 1.68×10^{44} erg s^{-1}, respectively, and a total gas mass of $M_{\rm gas} = 9.3 \times 10^{13}\ M_\odot$. These values put XLSSC-e at the average mass range of superclusters; its appearance, with two members of equal size, is quite unusual with respect to other superclusters and provides a unique view of the formation process of a massive structure.

Key words. galaxies: clusters: general – X-rays: galaxies: clusters

1. Introduction

Clusters of galaxies are promising tools that can be used to test cosmology and the predictions of General Relativity since they probe both the geometry of the universe and the growth of structure. The XXL project (Pierre et al. 2016, hereafter Paper I) is a large XMM survey at medium X-ray depth. It comprises two regions of 25 deg^2 each located on the celestial equator (XMM-LSS field) and on the southern hemisphere (BCS field). The main goal of XXL is to detect and use approximately

⋆ This work is based on observations obtained with *XMM-Newton*, an ESA science mission with instruments and contributions directly funded by ESA Member States and the USA (NASA) and on observations obtained at the WHT thanks to the International Time Programme (CCI) and the Opticon FP7 program. It also used observations made with ESO Telescopes at the La Silla Paranal Observatory under programme LP 191.A-0268.
⋆⋆ The Master Catalogue is available at the CDS via anonymous ftp to cdsarc.u-strasbg.fr (130.79.128.5) or via http://cdsarc.u-strasbg.fr/viz-bin/qcat?J/A+A/592/A2

500 galaxy clusters ($0 < z < 1$) to constrain the time evolution of the Dark Energy equation of state (Pierre et al. 2011).

Moreover, XXL provides an unprecedented volume between $0.5 < z < 1$ with which to study the nature and evolutionary properties of groups, clusters, and superclusters of galaxies. The formation of a web of galaxies and systems of galaxies is predicted in the current cosmological paradigm where galaxies and galaxy systems form because of the constant amplification of initially very small fluctuations in the matter density. Density perturbations on scales ranging from 100 h^{-1} Mpc down to 10 h^{-1} Mpc give rise to the largest systems of galaxies, the superclusters, ranging from rich, large super-clusters containing many massive clusters extending over 10–20 Mpc down to less massive structures containing groups and poor clusters of the order of 10^{13}–10^{14} $M_{\odot}$ each (e.g. Einasto et al. 2011, and references therein).

The superclusters, already decoupled from the *Hubble* flow, are not yet virialised, but most of them will collapse under the effect of gravity. At larger scales dynamical evolution proceeds at a slower rate and super-clusters have retained the memory of the initial conditions of their formation. Therefore they are important sites where we can directly witness the process of structure formation and evolution and the mass assembly to form clusters.

In this paper we analyse a supercluster of galaxies, XLSSC-e, at redshift $z \sim 0.43$, the highest redshift supercluster found in XXL. It was obtained as a result of a percolation analysis with a linking length of 35 Mpc applied to the sample of the 100 brightest clusters (hereafter XXL-100-GC[1]) detected in the XXL Survey (Pacaud et al. 2016, hereafter Paper II).

It is composed of six cluster-sized galaxy concentrations (the Abell radius, $R_{\rm Abell}$, is ~1.2 Mpc at the mean supercluster redshift). They have all been independently well detected as significantly extended X-ray sources; all of them belong to the class of C1 clusters, i.e. the most secure and uncontaminated detections in the XXL cluster sample (see Paper II); and three (XLSSC 083, XLSSC 084, XLSSC 085) are part of the 100 brightest XXL clusters. Below we describe the existing multiwavelength observations, the results obtained so far, and our conclusions. We adopted a cosmology where $\Omega_0 = 0.282$, $\Omega_\Lambda = 0.718$, $H_0 = 69.7$ km s^{-1}/Mpc, i.e. (WMAP9+BAO), plus constraints on H_0 from Cepheids and type I*a* supernovae, same as in Paper II.

2. Observations and data reduction

Based on a cluster search using photometric redshifts in the CFHTLS wide fields, Durret et al. (2011) identified one potential cluster at $z_{\rm phot} = 0.48$ located at RA = 32.7603, Dec = −6.1936, and ~6.55′ away from our XLSSC 085 cluster; this corresponds approximately to the position of the BCG of XLSSC 084.

From the XXL XMM observations, we have inferred, to date, the presence of five superclusters (Paper II). With a redshift of ~0.43, XLSSC-e – which is the subject of the present paper – is the most distant one. It consists of six X-ray emitting clusters arranged in a compact structure (~15′ × 30′), all components residing in a single XMM pointing.

Subsequent optical spectroscopy with the WHT (Koulouridis et al. 2016, hereafter Paper XII) confirmed the redshift of the structure.

[1] XXL-100-GC data are available in computer readable form via the XXL master catalogue browser: http://cosmosdb.iasf-milano.inaf.it/XXL

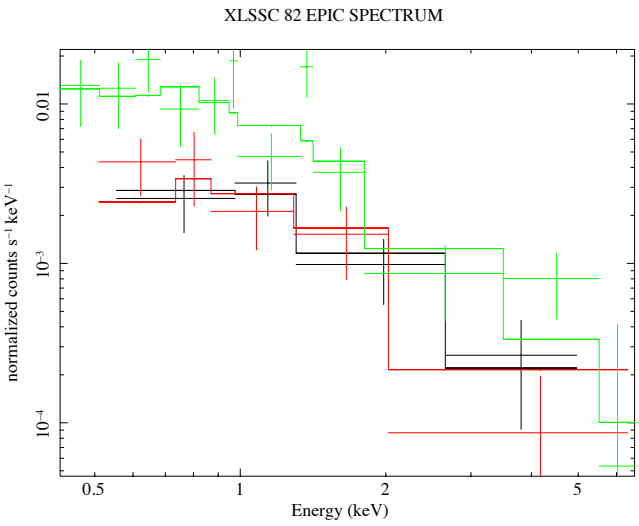

Fig. 1. X-ray spectra of the cluster XLSSC 082 taken from a 300 kpc aperture. The best fitting model is also shown. Data from MOS1, MOS2, and pn are plotted in black, red, and green, respectively.

2.1. X-ray observations

The data processing and the sample selection are fully described in Paper II. The spectral analysis performed to obtain temperature and luminosity measurements and the estimate of the mass are described in Giles et al. (2016, hereafter Paper III) and Lieu et al. (2016, hereafter Paper IV). These steps are briefly summarised here. The XXL observation was filtered by soft proton flares and images, exposure maps, and detector masks were generated and processed using the Xamin pipeline (Pacaud et al. 2006). Source detection and source extent were determined through a *SExtractor* run followed by a dedicated XMM maximum likelihood fitting procedure. To account for the background in the spectral analysis, local backgrounds taken at the same off-axis position as the cluster were used. Cluster spectra were extracted for each of the XMM cameras and fits performed in the 0.4–7.0 keV band with an absorbed APEC (Smith et al. 2001) model modified by Galactic absorption (Kalberla et al. 2005) and with a fixed metal abundance of 0.3 $Z_{\odot}$ (Anders et al. 1989). The statistic *cstar* was used and both source and background spectra were binned to 5 counts per bin at least (Willis et al. 2005). The typical X-ray spectrum is shown in Fig. 1.

The temperature ($T_{300\ \rm kpc}$) and luminosity (in the 0.5–2 keV band, $L^{\rm XXL}_{300\ \rm kpc}$) were derived within 300 kpc for each cluster as this radius is the largest radius for which a temperature could be derived for XXL-100-GC. The same aperture and procedure adopted for XXL-100-GC was used for the three clusters of XLSSC-e which are not in XXL-100-GC. As in Paper III, we adopted the $M_{\rm WL} - T$ relation derived in Paper IV to obtain the mass within an overdensity of 500 ($M_{500,\rm MT}$, M_{500} hereafter). Individual gas masses for each cluster were obtained following the method described in Eckert et al. (2016, hereafter Paper XIII). Namely, surface-brightness profiles were extracted from the X-ray peak after correcting for vignetting and subtracting the background. To obtain the gas mass, the profiles were deprojected assuming spherical symmetry, converted into density, and integrated over the volume. These quantities are reported for each cluster in Table 1.

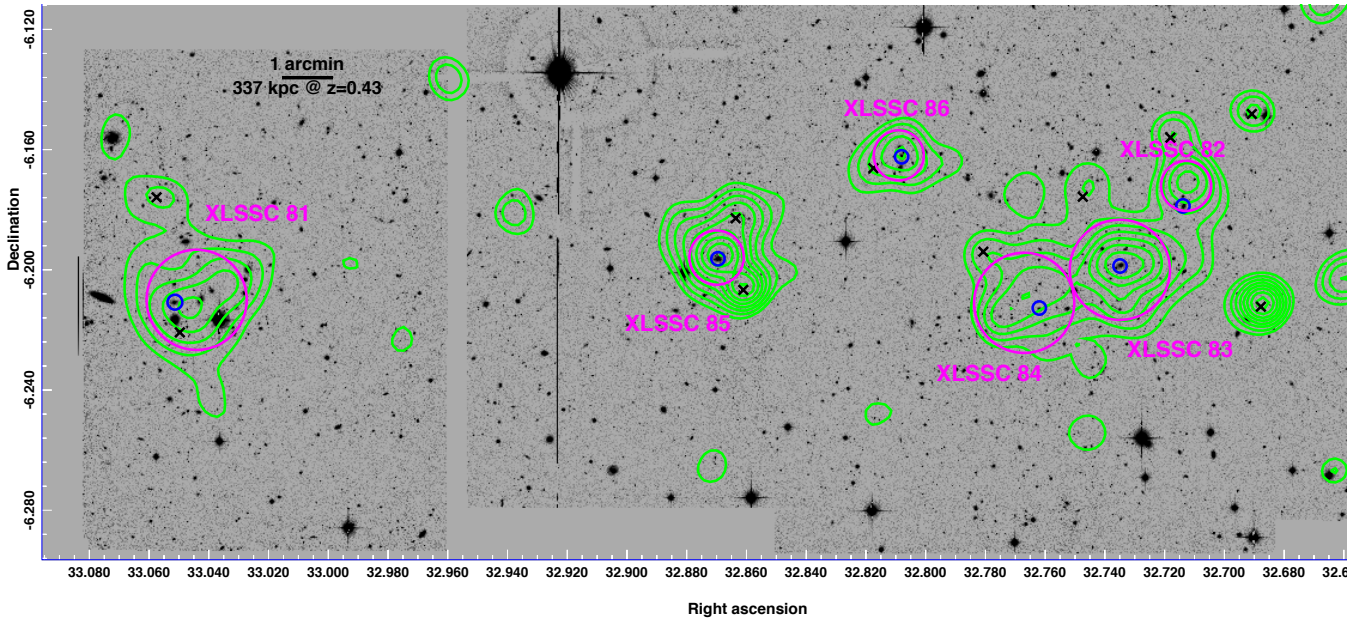

Fig. 2. CFHTLS MegaCam mosaic image in the *i* band with the X-ray contours superimposed in green; identified X-ray clusters are encircled in magenta circles, which have a radius $r = r_{500}$, and their XXL IDs indicated. The blue circles show the positions of the BCG in each cluster and the black crosses highlight the point sources excluded from the X-ray analysis. Contour levels are in logarithmic scale and they range from 4.5 counts/s/deg^2 to 30 counts/s/deg^2. North is up and east is on the left.

Table 1. Properties of XLSSC-e supercluster.

Group ID	Class	RA (J2000)	Dec (J2000)	$z_{\rm spec}$	$N_{\rm gal}$	$T_{300\ \rm kpc}$ keV	$L^{\rm XXL}_{300\ \rm kpc}$ 10^{43} erg s^{-1}	$L^{\rm XXL}_{500,\rm MT}$ 10^{43} erg s^{-1}	$M_{500,\rm MT}$ $10^{14}\ M_\odot$	$M_{\rm gas,500}$ $10^{13}\ M_\odot$
XLSSC 081	C1	33.044	–6.210	0.428 ± 0.001	5	$1.7^{+0.3}_{-0.2}$	1.49 ± 0.34	1.73 ± 0.39	0.7 ± 0.4	$1.5^{+0.4}_{-0.3}$
XLSSC 082	C1	32.714	–6.173	0.424 ± 0.002	4	$3.9^{+1.7}_{-0.6}$	1.71 ± 0.28	2.43 ± 0.40	2.9 ± 2.5	$1.1^{+0.2}_{-0.2}$
XLSSC 083	C1	32.735	–6.200	0.430 ± 0.004	3	$4.8^{+1.2}_{-0.9}$	3.13 ± 0.25	4.79 ± 0.39	4.1 ± 2.5	$1.4^{+0.3}_{-0.27}$
XLSSC 084	C1	32.767	–6.211	0.430 ± 0.002	4	$4.5^{+2.3}_{-1.5}$	1.38 ± 0.21	2.06 ± 0.32	3.7 ± 3.9	$1.7^{+0.5}_{-0.4}$
XLSSC 085	C1	32.870	–6.196	0.428 ± 0.003	4	$4.8^{+2.0}_{-1.0}$	2.83 ± 0.29	4.33 ± 0.44	4.1 ± 3.5	$2.7^{+0.5}_{-0.47}$
XLSSC 086	C1	32.809	–6.162	0.424 ± 0.001	5	$2.6^{+1.2}_{-0.6}$	1.12 ± 0.31	1.43 ± 0.40	1.5 ± 1.3	$0.9^{+0.4}_{-0.3}$

Notes. We list below the cluster ID, its classification according to the XXL convention, the coordinates of the centre of each cluster, the spectroscopic redshift, and the number of galaxies which contributed to the redshift measurement, the X-ray temperature within the 300 kpc aperture, the luminosity within the 300 kpc aperture and within r_{500} in the 0.5−2 keV band, the mass estimated using the XXL $M_{\rm WL} - T$ relation (Paper IV), and the gas mass estimated as in Paper XIII.

2.2. Optical observations

2.2.1. Photometry

The brightest cluster galaxy (BCG) for each cluster was identified by choosing the brightest galaxy in the MegaCam *z* filter within $r \leq 0.5 \times r_{500}$ of the X-ray emission centroid (see Lavoie et al., in prep., for the full catalog of BCGs in the full sample of the 100 brightest XXL clusters).

We corrected the *g* and *r* magnitudes for extinction following Schlegel et al. (1998) and we used *k* corrections from Chilingarian et al. (2010)[2]. Assuming an absolute solar magnitude of 4.67 in r, and neglecting correction for passive evolution, we calculated the *r* luminosity for each BCG; finally, we calculated their mass using the relation $\log(M_*/L_\odot) = -0.306 + 1.097 \times (g - r)$ from Bell et al. (2003).

[2] http://kcor.sai.msu.ru/

2.2.2. Spectroscopy

We observed the super-cluster with the 4.2 m *William Herschel* Telescope (WHT) during four nights in 2013 (29−30 October and 9−10 November) using the AutoFib2+WYFFOS (AF2) spectrograph with a fibre diameter of 1.6″, covering the spectral range from 3800 Å to 7000 Å, an instrumental resolution of 4.4 Å. We limited ourselves to the central 20′ to minimise the effects of vignetting. Exposure times were 2.5 h and 3.5 h for the bright ($19 \leq r_{\rm SDSS} \leq 20.5$) and faint targets ($20.5 \leq r_{\rm SDSS} \leq 21$), respectively. During this run fibres were allocated on the BCG galaxy of each structure, and the surrounding galaxies within 1 Mpc of each BCG; a total of 15 galaxies were confirmed spectroscopically as cluster members. Further details about the data reduction and analysis can be found in Paper XII.

The redshift of the galaxy identified as the BCG of XLSSC 084 and other additional member candidates (see Table 2) was obtained with NTT+EFOSC2, covering the spectral range from 5000 Å to 9300 Å with an instrumental resolution of 4.1 Å.

Table 2. Measured redshift and its associated error for each cluster member within $R = 1$ Mpc for XLSSC 081, XLSSC 085, XLSSC 086, and within $R = 500$ kpc for XLSSC 082, XLSSC 083, and XLSSC 084.

Cluster name	RA (2000)	Dec (2000)	z
XLSSC 081	33.03092	–6.21239	0.4217 ± 0.0006
	33.05433	–6.21797	0.4310 ± 0.0006
	33.07499	–6.16943	0.4365 ± 0.0008
	33.08085	–6.21790	0.4285 ± 0.0008
	33.05150	–6.21080	0.4266 ± 0.0004
XLSSC 082	32.69952	–6.17843	0.4310 ± 0.0003
	32.71404	–6.17883	0.4240 ± 0.0005
	32.71432	–6.17522	0.4239 ± 0.0004
	32.71715	–6.17787	0.4201 ± 0.0007
XLSSC 083	32.71678	–6.18519	0.4399 ± 0.0005
	32.73504	–6.19842	0.4298 ± 0.0005
	32.73862	–6.20253	0.4422 ± 0.0006
XLSSC 084	32.75402	–6.20126	0.4180 ± 0.0011
	32.76217	–6.21303	0.4324 ± 0.0005
	32.76234	–6.19310	0.4312 ± 0.0017
	32.77803	–6.21378	0.4286 ± 0.0011
XLSSC 085	32.86146	–6.18232	0.4283 ± 0.0007
	32.86293	–6.20681	0.4355 ± 0.0006
	32.86983	–6.19639	0.4288 ± 0.0005
	32.88399	–6.21361	0.4267 ± 0.0007
XLSSC 086	32.79592	–6.16700	0.4243 ± 0.0005
	32.79750	–6.19569	0.4310 ± 0.0005
	32.80875	–6.16600	0.4235 ± 0.0008
	32.80908	–6.15931	0.4235 ± 0.0005
	32.81446	–6.18642	0.4109 ± 0.0005

Notes. The choice of a different radius is dictated by the need to avoid overlapping between the last three clusters.

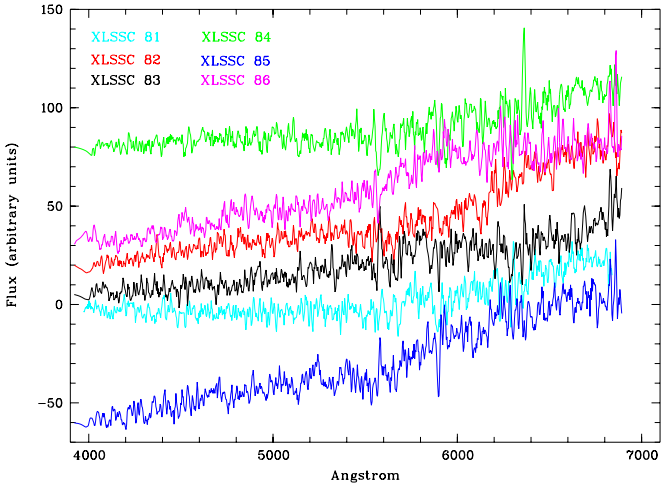

Fig. 3. Final reduced spectra of the BCG for all the clusters discussed here. Spectra have been shifted by arbitrary units to facilitate the viewing.

The relevant parameters for all the BCGs in the supercluster are shown in Table 3, while the final spectra are shown in Fig. 2.

We calculated the relative velocity of each cluster, assuming as the centre of the structure the BCG of XLSSC 085, the most massive cluster in the structure; we found that the other clusters move with a relative speed between 210 km s^{-1} and 840 km s^{-1} with an estimated error of the order of 95 km s^{-1}.

3. Results

From the data sets presented above, we can extract the following results:

- We are observing a supercluster with a multiplicity of 6 (we observe six distinct clusters of galaxies, each with its own BCG) with a total extent of 11 × 2.9 Mpc in the sky and 21 Mpc along the line of sight. The total X-ray derived mass is ∼1.7 × 10^{15} $M_{\odot}$, while the gas mass is $M_{\rm gas}$ = 9.3 × 10^{13} $M_{\odot}$. From the total estimated gas mass and total mass of the system, we infer an average gas fraction of ∼5% in the supercluster; this is typical of what we observe in XXL clusters, see Paper XIII.
- The optical appearance of four out of the six clusters seems undisturbed and the X-ray emission is centred on the BCG, as can be seen in Fig. 1. On the other hand, XLSSC 082 and, especially, XLSSC 084, show an elongated appearance on the sky, preferentially along the axis XLSSC 082-XLSSC 083-XLSSC 084. The X-ray emission in these three clusters shows a common envelope.
- Two of the BCGs, XLSSC 082 and XLSSC 084, show a large separation from the X-ray emission centroid at 149 kpc and 202 kpc respectively. An offset between the BCG and the average redshift of the cluster is also evident in the optical data for XLSSC 084 where we measure a velocity difference of 700 km s^{-1}, while this is not observed for XLSSC 082. This likely indicates that XLSSC 084 is in a merging state (see Adami 2000), as also suggested by its disturbed X-ray morphology.
- An estimate of the crossing time of the supercluster is $t_{\rm c}$ = 2.11 Gyr, while the average escape velocity is of the order of 3.5 × 10^{3} km s^{-1}.

4. Discussion and conclusions

XLSSC-e is currently the most massive and most distant supercluster of galaxies found in XXL. In the literature, starting from the original definition of superclusters (see Bachall 1984) there are several catalogues of superclusters, mostly based on optical data. Only in the last two years (see Chon et al. 2013) has a search for superclusters based purely on X-ray detection been pursued; it reaches out to $z \leq 0.4$, and we note that no supercluster with more than three members can be found beyond redshift $z \sim 0.2$, most likely because of the depth of the RASS survey. XXL is the second survey which has detected several superclusters of galaxies and gone beyond $z = 0.4$. As already highlighted in Paper II, the selection method used for XXL superclusters has the advantage of relying only on galaxy structures showing clear evidence of a deep potential well and further extend the volume used for such study ($z \geq 0.3$). Although a few isolated very high redshift superclusters are known (e.g. Gal et al. 2004), our work is the first attempt to systematically unveil superstructures up to $z \geq 0.5$ in a homogeneous X-ray sample.

If we compare our supercluster with the low redshift sample of Chon et al. (2013) we find that its X-ray luminosity (1.7 × 10^{44} erg s^{-1} in the 0.1–2.4 keV band relevant for the comparison) is close to the median of that sample; with respect to other supercluster at $z \geq 0.4$ (see Verdugo et al. 2012; Geach et al. 2011; Schirmer et al. 2011; Lubin et al. 2009; Kartaltepe et al. 2008; Tanaka et al. 2007) our object has a total mass (M_{200} obtained using a conversion of r_{200}/r_{500} = 1.52, Piffaretti et al. 2011) of 2.3 × 10^{15} $M_{\odot}$, again in the middle of the range of the few known objects (see e.g. Table 1 in Schirmer et al. 2011).

Table 3. Properties of the BCGs.

BCG Clus-no.	RA (2000)	Dec (2000)	z	$(g-r)$	M_r	Mass $10^{11}\ M_\odot$
XLSSC 081	33.0515	–6.21080	0.4266 ± 0.0006	1.53	–21.61	7.7
XLSSC 082	32.7140	–6.17883	0.4240 ± 0.0005	1.42	–21.76	6.7
XLSSC 083	32.7350	–6.19845	0.4303 ± 0.0007	1.59	–21.80	10.6
XLSSC 084	32.7621	–6.21303	0.4324 ± 0.0004	1.51	–21.04	4.2
XLSSC 085	32.8697	–6.19631	0.4289 ± 0.0008	1.56	–22.27	15.1
XLSSC 086	32.8081	–6.16231	0.4257 ± 0.0006	1.39	–21.51	4.9

Notes. We list the BCG group ID, their coordinates, the redshift for each galaxy, the observed colour (corrected for extinction), their absolute magnitude in r band, and mass derived from the analysis of the optical data. The mass was obtained using the $M - L$ relation from Bell et al. (2003); an uncertainty of 10% should be assumed on the mass estimate.

On the other hand, XLSSC-e tends to differ from other known superclusters at those redshifts: instead of having a massive central cluster with infalling filaments and smaller structures, it has almost two equal-sized objects, making it qualitatively different from the network around an already formed massive cluster such as RXJ 1347 (Verdugo et al. 2012). While it is very difficult to infer any dynamical information from such a small number of redshifts, if we put together the relatively small crossing time, the common X-ray emission of three members, and the measured gas fraction and mass, we can speculate that we are observing an un-relaxed structure with an ongoing merging between at least three of the member clusters. If nothing else intervenes to alter the system, and assuming that the estimated crossing time is a good estimate of the merging time, it is likely that the supercluster will have completely merged in ~2.5 Gyr and will resemble a massive cluster of galaxies similar to the most massive known clusters, such as RXJ 1347. The observed gas should be progressively heated up by gravitational collapse and should relax after a few dynamical timescales, thus creating a hot, luminous X-ray halo similar to the ones observed in local massive clusters.

Subsequent extensive spectroscopic follow-up and a kinematic analysis are needed to confirm this hypothesis and to study the galaxy population of this and other large structures discovered by XXL. A study of the surrounding environment of XLSSC-e has been already done by Baran et al. (2016, hereafter Paper IX) using photometric redshifts.

Acknowledgements. XXL is an international project based around an XMM Very Large Programme surveying two 25 deg^2 extragalactic fields at a depth of ~5×10^{-15} erg cm^{-2} s^{-1} in the [0.5–2] keV band for point-like sources. The XXL website is http://irfu.cea.fr/xxl. Multiband information and spectroscopic follow-up of the X-ray sources are obtained through a number of survey programmes, summarised at http://xxlmultiwave.pbworks.com/. The authors wish to acknowledge the support from the staff at WHT and La Silla; we also thank the French PNCG and the French-Italian PICS for financial support which made this work possible. F.P. acknowledges support from the DLR Verbunforschung grant 50 OR 1117 and from the DFG Transregional Program TR33. N.Ba. and V.Smo. acknowledge the funding by the European Union's Seventh Frame-work programs under grant agreements 333654 (CIG, "AGN feedback") and 337595 (ERC Starting Grant, "CoSMass"). Y.J. acknowledges support by FONDECYT grant No. 3130476.

References

Adami, C., & Ulmer, M. P. 2000, A&A, 361, 13
Anders, E., & Grevesse, N. 1989, Geochim. Cochim. Acta, 53, 197
Bachall, N. A., & Soneira R. M. 1984, ApJ, 277, 27
Baran, N., Smolčić, V., Milaković, D., et al. 2016, A&A, A&A, 592, A8 (XXL Survey, IX)
Bell, E., McIntosh, D. H., Katz, N., & Weinber, M. D. 2003, ApJS, 149, 289
Chilingarian, I. V., Melchior, A.-L., & Zolotukhin, I. Yu. 2010, MNRAS, 405, 1409
Chon, G., Boehringer, H., & Nowak, N. 2013, MNRAS, 429, 3272
Durret, F., Adami, C., Cappi, A., Maurogordato, S., et al. 2011, A&A, 535, A65
Eckert, D., Ettori, S., Coupon, J., et al. 2016, A&A, 592, A12 (XXL Survey, XIII)
Einasto, M., Liivamaegi, L. J., Tago, E., et al. 2011, A&A, 532, A5
Gal, R. R., & Lubin, L. M. 2004 ApJ, 607, L1
Geach, J. E., Ellis, R. S., Smail, I., Rawle, D., & Moran, S. 2011, MNRAS, 413, 177
Giles, P. A., Maughan, B. J., Pacaud, F., et al. 2016, A&A, 592, A3 (XXL Survey, III)
Kalberla, P. M. W., Burton, W. B., Hartmann, D., et al. 2005, A&A, 440, 775
Kartaltepe, J. S., Ebeling, H., Ma, C. J., & Donovan, D. 2008, MNRAS, 389, 1240
Koulouridis, E., Poggianti, B., Altieri, B., et al. 2016, A&A, 592, A11 (XXL Survey, XII)
Lieu, M., Smith, G. P., Giles, P. A., et al. 2016, A&A, 592, A4 (XXL Survey, IV)
Lubin, L. M., Gal, R. R., Lemaux, B. C., Kocevski, D. D., & Squires, G. K. 2009, AJ, 137, 4867
Pacaud, F., Pierre, M., Refregier, A., et al. 2006, MNRAS, 372, 578
Pacaud, F., Clerc, N., Giles, P. A., et al. 2016, A&A, 592, A2 (XXL Survey, II)
Pierre, M., Pacaud, F., Juin, J. B., et al. 2011, MNRAS, 414, 1732
Pierre, M., Pacaud, F., Adami, C., et al. 2016, A&A, 592, A1 (XXL Survey, I)
Piffaretti, R., Arnaud, M., Pratt, G. W., et al. 2011, A&A, 534, A109
Schirmer, M., Hildebrandt, H., Kuijken, K., & Erben, T. 2011, A&A, 532, A57
Schlegel, D. J., Finkbeiner, D. P., & Davis, M. 1998, ApJ, 500, 525
Smith, R. K., Brickhouse, N. S., Liedahl, D. A., & Raymond, J. C. 2001, ApJ, 556, L91
Tanaka, M., Hoshi, T., Kodama, T., & Kashikawa, N. 2008 MNRAS, 379, 1546
Verdugo, M., Lerchster, M, Boehringer, H., et al. 2012, MNRAS, 421, 1949
Willis, J. P., Arnaud, M., Pratt, G. W., et al. 2005, MNRAS, 363, 675